

Behavioral pattern separation and its link to the neural mechanisms of fear generalization

Iris Lange,¹ Liesbet Goossens,¹ Stijn Michielse,¹ Jindra Bakker,¹ Shmuel Lissek,² Silvia Papalini,³ Simone Verhagen,¹ Nicole Leibold,¹ Machteld Marcelis,^{1,4} Marieke Wichers,⁵ Ritsaert Lieverse,¹ Jim van Os,^{1,6} Therese van Amelsvoort,¹ and Koen Schruers^{1,7}

¹Department of Psychiatry and Psychology, School of Mental Health and Neuroscience, EURON, Maastricht University Medical Centre, Maastricht, The Netherlands, ²Department of Psychology, University of Minnesota, Minneapolis, MN, USA, ³Donders Institute for Brain, Cognition and Behaviour, Centre for Cognitive Neuroimaging, Radboud University, Nijmegen, The Netherlands, ⁴Institute for Mental Health Care Eindhoven (GGzE), Eindhoven, The Netherlands, ⁵Department of Psychiatry, Interdisciplinary Center Psychopathology and Emotion Regulation (ICPE), University of Groningen, University Medical Center Groningen, Groningen, The Netherlands, ⁶Department of Psychosis Studies, Institute of Psychiatry, King's College London, King's Health Partners, London, UK, and ⁷Faculty of Psychology, Center for Experimental and Learning Psychology, University of Leuven, Leuven, Belgium

Correspondence should be addressed to Iris Lange, Department of Psychiatry and Psychology, Maastricht University Medical Centre, P.O. Box 616, 6200 MD, Maastricht, The Netherlands. E-mail: i.lange@maastrichtuniversity.nl

Abstract

Fear generalization is a prominent feature of anxiety disorders and post-traumatic stress disorder (PTSD). It is defined as enhanced fear responding to a stimulus that bears similarities, but is not identical to a threatening stimulus. Pattern separation, a hippocampal-dependent process, is critical for stimulus discrimination; it transforms similar experiences or events into non-overlapping representations. This study is the first in humans to investigate the extent to which fear generalization relies on behavioral pattern separation abilities. Participants ($N = 46$) completed a behavioral task taxing pattern separation, and a neuroimaging fear conditioning and generalization paradigm. Results show an association between lower behavioral pattern separation performance and increased generalization in shock expectancy scores, but not in fear ratings. Furthermore, lower behavioral pattern separation was associated with diminished recruitment of the subcallosal cortex during presentation of generalization stimuli. This region showed functional connectivity with the orbitofrontal cortex and ventromedial prefrontal cortex. Together, the data provide novel experimental evidence that pattern separation is related to generalization of threat expectancies, and reduced fear inhibition processes in frontal regions. Deficient pattern separation may be critical in overgeneralization and therefore may contribute to the pathophysiology of anxiety disorders and PTSD.

Key words: behavioral pattern separation; perceptual discrimination; fMRI; fear generalization; neurobiology

Received: 6 October 2016; Revised: 4 August 2017; Accepted: 6 September 2017

© The Author (2017). Published by Oxford University Press.

This is an Open Access article distributed under the terms of the Creative Commons Attribution Non-Commercial License (<http://creativecommons.org/licenses/by-nc/4.0/>), which permits non-commercial re-use, distribution, and reproduction in any medium, provided the original work is properly cited. For commercial re-use, please contact journals.permissions@oup.com

Introduction

Fear generalization is an adaptive mechanism, as it enables an individual to appropriately respond to novel, but possibly harmful stimuli based on overlapping features with a learned threat stimulus. It can however become maladaptive when an individual fearfully responds to environmental cues that actually convey safety. This is called overgeneralization, and it has been suggested to represent a phenotypic marker of anxiety disorders and post-traumatic stress disorder (PTSD) (Lissek 2012; Kaczurkin et al., 2016). If overgeneralization of fear occurs in many day-to-day situations, it can severely impact on daily functioning (Dymond et al., 2014; Dunsmoor and Paz, 2015). In addition, it may give rise to enhanced instrumental avoidance behavior (van Meurs et al., 2014), thereby contributing to pathological behaviors and preventing the disconfirmation of maladaptive associations. Comprehending the complexity of fear generalization by studying its neural circuitry and underlying mechanisms contributes to neurobiological insight into clinical anxiety and may assist in developing novel treatment options.

Recent neuroimaging studies have begun to elucidate the neural mechanisms of fear generalization (Greenberg et al., 2013a; Dymond et al., 2014; Dunsmoor and Paz, 2015; Onat and Büchel, 2015; Lopresto et al., 2016). Experimental designs typically include multiple generalization stimuli (GS) that become increasingly similar to a threat stimulus. Both behavioral and psychophysiological responses follow a generalization gradient linked to the perceptual overlap. Brain areas involved in threat processing, including the anterior insula, dorsal anterior cingulate cortex (dACC), thalamus/periaqueductal gray, caudate and ventral tegmental area (VTA), show positive generalization gradients, with higher activation to stimuli with increasing resemblance to a threat stimulus. Negative gradients, with decreasing activation to stimuli with a higher resemblance to a threat stimulus, have been observed in regions involved in fear inhibition and self-consciousness, such as the ventromedial prefrontal cortex (vmPFC), and precuneus (Lissek et al., 2013; Dunsmoor and Paz, 2015; Onat and Büchel, 2015). Furthermore, both animal studies and human imaging studies point to the importance of the hippocampus in fear generalization (Lissek et al., 2013; Xu and Südhof, 2013; Cullen et al., 2015). It has been proposed that this is due to involvement of hippocampal subfields in the process of pattern separation and completion (Kheirbek et al., 2012; Lissek, 2012; Lissek et al., 2013; Besnard and Sahay, 2015; Dunsmoor and Paz, 2015).

Pattern separation is a computational process separating features of similar sensory inputs into distinct memory representations. As a result, interference between an incoming new input and previously stored information is minimized (Besnard and Sahay, 2015). Due to the perceptual process of pattern separation, a person can make a distinction between seemingly similar stimuli or experiences. Pattern completion refers to a process retrieving memory patterns from partial external cues (Li et al., 2010). A series of animal and human neuroimaging studies have shown that these complementary computational processes engage different hippocampal subregions, with the dentate gyrus (DG) being involved in pattern separation, and the cornu ammonis 3 promoting both pattern separation and completion, depending on proximity to the DG and input dissimilarity (Bakker et al., 2008; Aimone et al., 2011; Sahay et al., 2011; Yassa and Stark, 2011; Nakashiba et al., 2012; Deuker et al., 2014; Neunuebel and Knierim, 2014).

Due to its involvement in stimulus discrimination, pattern separation has also been proposed to play a critical role in

discrimination of safety stimuli that show some similarities to threatening stimuli (Kheirbek et al., 2012). More specifically, the process of pattern separation stores input from a novel, safe context into a distinct representation from the original threatening memory. In this way, a similar (but safe) stimulus can be discriminated from a threat stimulus. Pattern separation processes are thought to engage fear inhibition regions in this instance, including the vmPFC. However, if pattern separation fails and pattern completion is initiated, the safe stimulus activates the representation of the threat stimulus memory, resulting in the recruitment of threat-processing regions (Lissek et al., 2013; Dymond et al., 2014). Therefore, deficits in the process of pattern separation may result in overgeneralization (Kheirbek et al., 2012; Dymond et al., 2014; Besnard and Sahay, 2015). Hence, impaired pattern separation could substantially contribute to clinical anxiety, providing a powerful rationale to further examine the link between pattern separation and fear generalization. Although animal studies have demonstrated that fear discrimination requires pattern separation in the DG (McHugh et al., 2007; Sahay et al., 2011), human studies are lacking.

This study is the first experimental study in humans to examine the link between behavioral pattern separation abilities and the behavioral and neural mechanisms of fear generalization. We recruited healthy volunteers who underwent both a validated, non-emotional behavioral task taxing pattern separation mechanisms and an fMRI fear generalization paradigm. We hypothesized that lower behavioral pattern separation would be linked to enhanced generalization in behavioral ratings. Furthermore, it was hypothesized that lower behavioral pattern separation can be linked to lower recruitment of fear inhibition regions and enhanced reactivity of the neural fear network when processing GS. In addition, as previous studies have shown, the prediction was to find positive generalization gradients in brain regions involved in threat processing, and negative gradients in regions involved in fear inhibition (Lissek et al., 2013).

Materials and methods

Participants

Healthy adolescents and young adults aged 16–25 were recruited as part of the SmartsScan project (Dutch Trial Register Number: NTR3808). SmartsScan is a large-scale randomized controlled trial exploring the effects of psychological treatment for subclinical psychiatric symptoms on reward and fear learning phenotypes and related neurobiological mechanisms. This study included baseline data of forty-six individuals [mean age = 20.7 (SD = 2.2); N female/male = 36/10; educational level (N lower secondary/higher secondary/professional or university) = 3/2/41]. Exclusion criteria were current psychiatric diagnosis, as assessed with the MINI International Neuropsychiatric Interview (Overbeek et al., 1999), previous psychiatric treatment, current drug/alcohol abuse, use of psychoactive medication, a history of neurological disorder and MRI contra-indications. Before study participation, written informed consent was obtained from all individuals, and from parents when age of the individual was below 18 years. The study was approved by the local ethics committee.

Pattern separation task

Behavioral pattern separation performance was assessed with the mnemonic similarity task (MST) (Stark et al., 2013). During

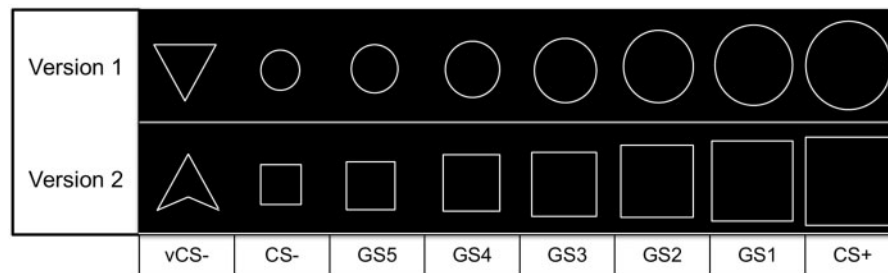


Fig. 1. Conditioned stimuli (vCS⁻, CS⁻, CS⁺) and generalization stimuli (GS1–GS5). As presented here, the largest circle/rectangle served as the CS⁺, the smallest circle/rectangle served as the CS⁻ for half of the subjects. For the other half of the subjects, the smallest circle/rectangle served as the CS⁺, and the largest circle/rectangle as the CS⁻.

the encoding phase, participants viewed 128 object images on a computer screen and classified these images as either indoor or outdoor objects via button responses. Stimulus presentation was 2 s, the inter-stimulus interval (ISI) 0.5 s. Immediately after the encoding phase, a retrieval phase started, during which 192 object images were presented that were either completely new images (64 images), exactly the same (64 images), or similar to the images presented during the encoding phase (64 images). Participants were asked to correctly classify these images as new (foil), old (target) or similar (lure) items (see Supplementary Figure S1 for a task overview). Duration of the encoding phase was 5.3 min, and the retrieval phase 8 min.

The lure discrimination index (LDI) is the main outcome measures and is calculated as the percentage correct ‘similar’ responses to lure items, and is corrected for biased responding towards ‘similar’ by subtracting the percentage of ‘similar’ responses to foils. A higher LDI reflects better behavioral pattern separation performance. The task also provides a traditional recognition memory score, calculated as the percentage correct ‘old’ responses to targets, with response bias correction for ‘old’ by subtracting percentage of ‘old’ responses to foils. Similarly, a higher traditional recognition score reflects better general recognition abilities.

FMRI fear generalization task

The experimental task to measure fear generalization was similar to a previously published protocol (Lissek et al., 2013).

Stimuli. Stimuli were seven rings or rectangles of parametrically increasing sizes, and a triangle (see Figure 1). The conditioned stimuli (CS⁺ and CS⁻) were the largest and smallest rings/rectangles. For half of the subjects, the largest ring/rectangle was the CS⁺ and the smallest ring/rectangle the CS⁻; for the other half this was reversed. The triangle served as a second CS⁻ (vCS⁻), as measure independent of generalization. The five intermediately sized rings/rectangles served as GS (GS1–GS5). GS1 was most similar and GS5 least similar to the CS⁺. A fixation cross was shown all times. Stimulus presentation was 4.4 s; the ISI was either 2.2 or 4.4 s.

The unconditioned stimulus (US) was an electrical pulse of 200 ms delivered to the left inner ankle (Biopac Systems, Inc., USA). Prior to experiment onset, shock intensity was calibrated so that all participants rated the shock as ‘highly uncomfortable but not painful’. Shock intensity varied between (2 and 50 mA), with an average shock intensity of 24.3 mA (SD = 15.9). The US co-terminated with the CS⁺.

Design. The task consisted of (1) a pre-conditioning phase, in which all stimuli were shown, (2) a conditioning phase with

only the CS⁺, CS⁻, vCS⁻ and (3) a generalization phase in which all stimuli presented. Stimuli were presented 12 times per task phase. The US co-terminated in 8/12 occurrences (66% reinforcement) with the CS⁺ during conditioning, and in 6/12 occurrences (50% reinforcement) during generalization. The sequence of stimuli was quasi-random; the same stimulus was not presented more than twice consecutively. Each phase was divided into two blocks in order to establish an even stimulus distribution. A genetic algorithm for optimizing experimental task designs (Wager and Nichols, 2003) was used to establish the sequence. The duration of the pre-conditioning and generalization phase was 12.4 min, while the duration of the conditioning phase was 4.7 min. All task phases were conducted on the same day.

Behavioral ratings. In order to track expectancies of receiving a shock, participants were asked four times per stimulus type to rate shock expectancy on a 4-point scale during each task phase (1 = no risk; 2 = low risk; 3 = moderate risk; 4 = high risk of receiving a shock), when the color of the fixation cross changed from white to red (for 880 ms). To restrict the number of subjective ratings during stimulus presentation, and not confound different subjective measures, participants were asked to rate their fear for the presented stimuli after each task phase. Level of fear was measured on a visual analogue scale ranging from 0 (no fear) to 100 (high fear). Furthermore, valence and arousal were rated.

Task instructions. Before onset of the task, participants were instructed to attend to the presented stimuli and learn to predict the shock. Furthermore, the button box responses for the behavioral ratings were practiced.

MRI acquisition and preprocessing

MRI scans were acquired using a 3 T Siemens Magnetom Prisma system (Siemens Healthcare, Erlangen, Germany) equipped with a 64-channel head/neck coil. T1-weighted Magnetization Prepared Rapid Acquisition Gradient Echo (MPRAGE) images with a voxel size of 1 mm × 1 mm × 1 mm were acquired (repetition time (TR) = 2250 ms, echo time (TE) = 2.21 ms, flip angle = 9°, field of view (FOV) = 256 × 256 × 192, sagittal slice orientation, GRAPPA = 2) to serve as anatomical reference. Functional scans were acquired using a T2*-weighted echoplanar images (EPIs) sequence (TR = 2450 ms, TE = 28 ms, flip angle = 75°, interleaved, FOV = 216 mm, axial orientation, GRAPPA = 3) with a voxel size of 3 mm × 3 mm × 3 mm. During the pre-conditioning and generalization phase, 303 volumes were acquired. During the acquisition phase, 114 volumes were acquired.

Functional magnetic resonance imaging data processing and analyses were carried out using FEAT (FMRI Expert Analysis Tool) of FSL (FMRIB's Software Library) version 5.0.6 (Smith et al., 2004). Pre-processing included non-brain removal (BET) (Smith, 2000), motion correction using MCFLIRT with the middle volume as reference (Jenkinson et al., 2002), high-pass temporal filtering with a cut-off of 100 s, spatial smoothing with a Gaussian kernel of 6 mm FWHM, pre-whitening (Woolrich et al., 2001), co-registration using FLIRT (Jenkinson et al., 2002) and normalization into Montreal Neurological Institute 152 stereotaxic space (MNI) using FNIRT for non-linear registration (Andersson et al., 2007).

Data analyses

Behavioral fear generalization gradients and pattern separation. Behavioral data of the pre-conditioning were analyzed with repeated measures ANOVA with stimulus type as within subject factor, using Greenhouse-Geisser correction when required, and pairwise post-hoc comparisons (Bonferroni corrected). Conditioning effects were tested by a stimulus type (vCS^- , CS^- , CS^+) \times time (pre-conditioning, post-conditioning) ANOVA.

Generalization effects in fear and shock expectancy scores were similarly analyzed with repeated measures analyses, using stimulus type (from vCS^- , CS^- , GS5-1, to CS^+) as within-subject factor, and additional testing for linear and quadratic components using Stata 13 (StataCorp 2013). To examine the association between LDI and generalization, correlation analyses were run with LDI and the following continuous behavioral fear generalization outcomes:

1. The difference between the CS^+ and GS1, the most similar GS.
2. Departure from linearity of the generalization gradient, as previously described by van Meurs et al. (2014): Linearity of the generalization curve reflects increased generalization. The average of the CS^+ and CS^- is the theoretical midpoint of a linear curve. The degree of linearity was calculated as the average of GS1–GS5 minus the average of the CS^+ and CS^- . Positive scores reflect positive departure from linearity (above the midpoint) and negative scores reflect negative departure from linearity (below midpoint), which correspond to enhanced or decreased generalization, respectively.

Furthermore, in order to test whether fear generalization cannot be explained by general recognition abilities, we also ran correlation analyses between the traditional recognition outcome and LDI, and the traditional recognition outcome and the generalization measures.

MRI analyses. First-level general linear models were computed for each participant. These models included eight explanatory variables (EVs) for the stimuli (CS^+ , vCS^- , CS^- , GS1, GS2, GS3, GS4 and GS5), and covariates of no interest including shock onset, motion parameters, and motion outliers as measured with the FSL motion outliers program. Individual activation maps were created for all stimuli. Contrasts of parameter estimates for $CS^+ > vCS^-$ and $vCS^- > CS^+$ were created to establish brain regions involved in threat and safety processing respectively. The contrasts $CS^+ > GS1$ and $CS^+ > \text{average}(GS1-GS5)$ were created as measures of fear generalization.

At the group-level, we first assessed which brain regions show threat-related or safety-related activations. The contrasts $CS^+ > vCS^-$ and $vCS^- > CS^+$ were analyzed with FEAT with mixed effects (FLAME) and cluster significance of $Z > 2.3$ and

$P < 0.05$ with Gaussian Random Field (GRF) correction for multiple comparisons. Significant regions previously reported to be involved in fear generalization were defined as regions of interest (ROIs) (Dunsmoor and Paz, 2015): insula, ACC, thalamus, caudate, VTA, vmPFC, precuneus and hippocampus. The probabilistic Harvard–Oxford atlases (thresholded at 20%) were used for anatomic labeling and masking. The VTA was identified, based on previous literature (Cha et al., 2014), by a 4 mm radius sphere around MNI [$3 -17 -12$]. In these functional ROIs, we extracted percent signal change per stimulus type using FeatQuery. To assess generalization gradients in these regions, repeated measures analyses were conducted with Greenhouse-Geisser correction when required, and additional tests for linear and quadratic trends. Generalization gradients outside these ROIs were subsequently analyzed in a similar way.

To investigate the link between behavioral generalization and neural activations, we ran regression analyses with FLAME using the generalization contrasts $CS^+ > GS1$ and $CS^+ > \text{average}(GS1-GS5)$, and corresponding behavioral measures as independent variables. The contrast $CS^+ > \text{average}(GS1-GS5)$ reflects a broader form of generalization to all GS. The relationship between behavioral pattern separation and the neural correlates of fear generalization was subsequently assessed with the same generalization contrasts, with LDI as predictor. All analyses were run with pre-threshold masking to restrict analyses to our ROIs, and whole-brain. A statistical threshold of $Z > 2.3$ and cluster-corrected threshold of $P < 0.05$ with GRF-correction for multiple comparisons were applied.

Psycho-physiological interactions (PPI) analyses

A subsequent exploratory PPI analysis was run to assess functional connectivity between the cluster showing associations with LDI (subcallosal cortex; see Results) and other brain regions. The time course of the seed region (a 5-mm sphere around the peak of the subcallosal cluster) was entered into a whole-brain PPI analysis together with the psychological regressor [contrast $CS^+ > \text{average}(GS1-GS5)$], and the PPI term. Z statistic images were thresholded less strictly at $Z > 2.0$ with a cluster threshold of $P < 0.05$, with GRF-correction for multiple comparisons.

Results

Behavioral pattern separation data

The LDI reflecting behavioral pattern separation performance was similar to previously reported data ($M = 40.21$, $SD = 14.48$) (Stark et al., 2013). This was also the case for the traditional recognition score ($M = 79.73$, $SD = 25.97$). Table 1 shows response proportions for each stimulus (target, lure, foil) and response type (old, similar, new). As expected based on previously reported data (Stark et al., 2013), participants frequently correctly identified targets and foils (respectively, $M = 84.62$, $SD = 16.42$; $M = 85.54$, $SD = 16.59$), while lures were less frequently correctly classified ($M = 49.67$, $SD = 12.96$), being classified as an old object instead ($M = 41.33$; $SD = 14.21$). No significant association was found between LDI and the traditional recognition score ($r = 0.22$, $P = 0.15$).

Behavioral generalization gradients. After pre-conditioning, fear scores were similar across stimuli ($F(7,308) = 1.163$, $P = 0.32$ (see Figure 2). Successful conditioning was reflected by a significant stimulus type \times time (pre-conditioning, post-conditioning)

interaction effect, with post-hoc testing showing that fear ratings significantly increased for CS⁺ from pre-to-post conditioning compared with the vCS⁻ ($F(1,44) = 121.92, P < 0.0001$) and CS⁻ ($F(1,44) = 119.51, P < 0.0001$). There were no differences in change from pre-to-post conditioning for the fear scores between the vCS⁻ and CS⁻ ($F(1,44) = 0.00, P = 1.00$).

Fear scores obtained after the generalization phase followed an increasing gradient from vCS⁻ toward CS⁻, GS5–GS1 to the CS⁺ ($F(3.92,176.24) = 103.44, P < 0.0001$), with significant linear and quadratic components [linear: $F(1,45) = 277.74, P < 0.0001$; quadratic: $F(1,45) = 53.61, P < 0.0001$] (see Figure 2). Post-hoc comparisons showed that fear scores of the CS⁺, and GS1–GS4 were higher than the fear score of vCS⁻ [all $t(40) > 5.18, P < 0.001$]. Fear ratings were similar for the CS⁺ and the most similar GS (GS1) ($P = 0.44$). Similarly, the shock expectancy scores displayed a generalization gradient with linear and quadratic components [$F(3.61, 158.74) = 117.34, P < 0.0001$; linear: $F(1,45) = 288.84, P < 0.001$; quadratic: $F(1,45) = 104.74, P < 0.001$].

Table 1. Results of the behavioral pattern separation task

	Target	Lure	Foil
Old	84.62 ± 16.42	41.33 ± 14.21	3.22 ± 4.16
Similar	10.53 ± 9.12	49.67 ± 12.96	9.44 ± 9.58
New	4.89 ± 10.44	9.00 ± 9.89	85.54 ± 16.59

Percent responses per stimulus type and response type are presented. dACC=dorsal anterior cingulate cortex; VTA=ventral tegmental area; avmPFC= anterior ventromedial prefrontal cortex.

Post-hoc comparisons showed that, similarly to the fear scores, shock expectancy scores of the CS⁺, and GS1–GS4 were higher than the vCS⁻ [all $t(40) > 3.95, P < 0.05$]. However, the gradient seemed to show a lower generalization pattern, as differences existed between the CS⁺ and GS1 [$t(40) = 6.93, P < 0.001$].

Link between behavioral pattern separation and subjective fear generalization

For the shock expectancy scores, analyses revealed that LDI was positively associated with CS⁺ > GS1 differentiation ($r = 0.298, P = 0.049$), and negatively associated with the linear departure score ($r = -0.355, P = 0.018$), indicating that higher behavioral pattern separation performance was linked to lower generalization in shock expectancy scores. No associations, however, were found between LDI and the fear CS⁺ > GS1 score ($r = 0.088; P = 0.567$), and the LDI and the fear linear departure score ($r = -0.10; P = 0.950$), reflecting absence of associations between behavioral pattern separation and generalization in fear ratings. The data did not reveal any significant associations between traditional recognition memory and the fear generalization outcomes (all $P > 0.35$).

Neural correlates of fear generalization

Expected regions showed threat-related activity (contrast CS⁺ > vCS), including the bilateral insula, dACC, thalamus and VTA (Figure 3 and Table 2). Significant regions outside the ROIs included the cerebellum, supramarginal gyri, dorsolateral PFC (dlPFC) and supplementary motor cortex

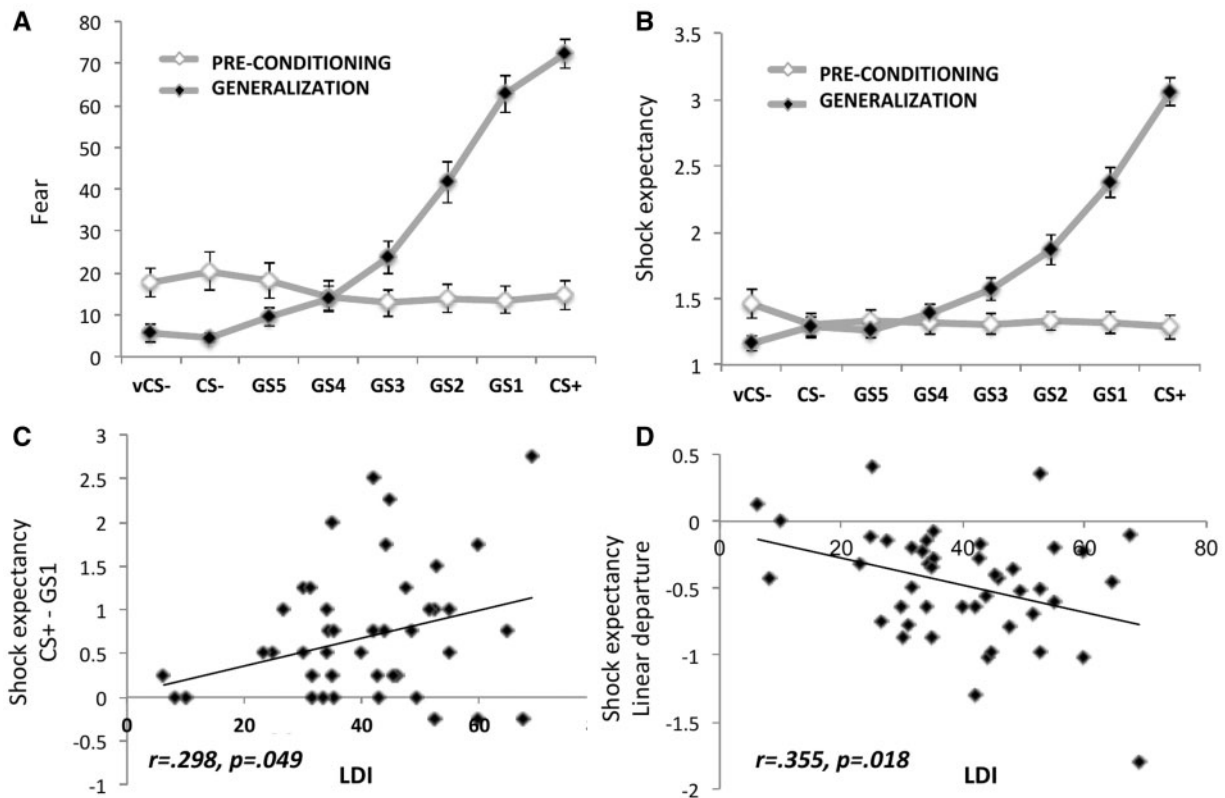


Fig. 2. Behavioral ratings and the associations between generalization measures and behavioral pattern separation (LDI) performance. (A) Fear ratings after the pre-conditioning and fear generalization phase. Values represent mean (SEM). (B) Shock expectancy ratings during the pre-conditioning and fear generalization phase. Values represent mean (SEM). (C) Correlation between behavioral pattern separation score (BPS) and fear generalization outcome 1: CS⁺–GS1 shock expectancy difference score. (D) Correlation between behavioral pattern separation (LDI) and fear generalization outcome 2: the linear departure score for shock expectancy.

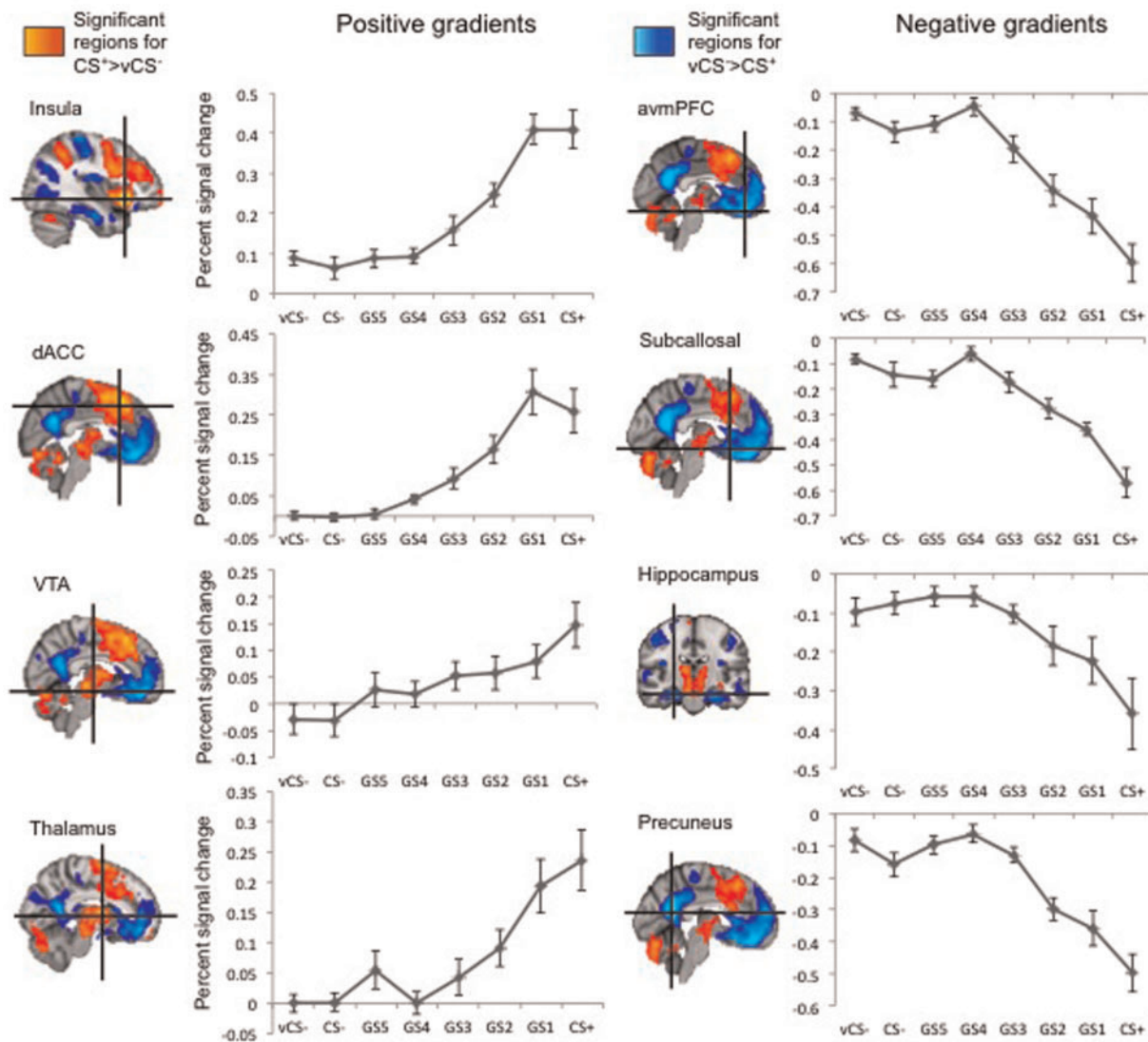


Fig. 3. Generalization gradients in the functional regions of interest. Values represent mean (SEM). Positive gradients were found in the dorsal anterior cingulate cortex (dACC), anterior insular cortex, VTA and thalamus. Negative generalization gradients were found in avntromedial prefrontal cortex (avmPFC), subcallosal cortex, hippocampus and precuneus.

(Messman-Moore et al., 2010) (Supplementary Table S1). Within the ROIs, positive gradients, with gradual increases from the vCS⁻ to the GS5–GS1 and CS⁺, were observed (Figure 3). The insula and thalamus displayed linear and quadratic components, while the neural activation curves in the VTA and dACC only revealed linear components, reflecting heightened generalization (Table 2). Generalization gradients were also observed in the other regions showing threat-related activity (Supplementary Figure S1 and Supplementary Table S3).

For the contrast vCS⁻ > CS⁺, safety-related activation was found in the bilateral hippocampi, in the vmPFC with peaks in different subregions, i.e. the subcallosal cortex and the anterior vmPFC (avmPFC), and precuneal cortex (Figure 3 and Table 2). Activation outside these ROIs was observed in the bilateral lateral occipital lobes and middle temporal gyri (Supplementary Table S2). Negative gradients, with gradual decrease from the vCS⁻ to the GS5–GS1 and CS⁺, were observed in all ROIs (Figure 3). All regions showed both linear and quadratic trends (Table 2). The middle temporal gyri and lateral occipital lobes showed

a similar pattern (Supplementary Figure S1 and Supplementary Table S3).

Correlation between behavioral and neural fear generalization

The regression analyses testing which ROIs display a similar generalization pattern as the behavioral data showed a positive association between shock expectancy CS⁺ > GS1 and activation in the left insula for the contrast CS⁺ > GS1 ([-30 18 -10], $Z = 3.51$, $r = 0.32$). No results were found for fear scores or regression analyses using the fMRI contrast CS⁺ > GS1–GS5.

Pattern separation and neural generalization

fMRI ROI-analyses revealed a negative correlation between the LDI and activation in the subcallosal cortex for the contrast CS⁺ > GS1–GS5 ([220 -4], $Z = 3.73$; $r = 0.42$), suggesting that higher pattern separation was associated with a higher neural

Table 2. Linear and quadratic components in brain regions showing generalized responses

	MNI coordinates	Z-value	F-test generalization gradient	Linear component	Quadratic component
Threat-related regions					
CS ⁺ > vCS ⁻					
Insula	l -28 20 -6	6.27	F(4.85,203.76) = 23.5; P < 0.0001	F(1,43) = 89.6 P < 0.0001	F(1,43) = 17.1, P < 0.0001
	r 38 20 -6	6.37	F(7,301) = 33.4, P < 0.0001	F(1,43) = 146.9, P < 0.0001	F(1,43) = 31.5, P < 0.0001
dACC	r 4 22 42	4.64	F(5.02,210.96) = 19.3, P < 0.0001	F(1,43) = 81.7, P < 0.0001	F(1,43) = 2.2, P = 0.146
	r 6 -16 -14	3.9	F(4.86,159.78) = 4.6, P < 0.01	F(1,43) = 21.94 P < 0.0001	F(1,43) = 1.3, P = 0.265
Thalamus	r 10 0 8	5.5	F(7,301) = 11.0, P < 0.0001	F(1,43) = 69.1 P < 0.0001	F(1,43) = 6.5, P < 0.05
Safety-related regions					
vCS ⁻ > GS ⁺					
vmPFC	l -2 40 -20	6.59	F(4.63,194.55) = 30.6, P < 0.0001	F(1,43) = 105.4, P < 0.0001	F(1,43) = 28.4, P < 0.0001
Subcallosal cortex	l -3 32 -22	6.28	F(4.38,183.84) = 23.9, P < 0.0001	F(1,43) = 61.5, P < 0.0001	F(1,43) = 35.5, P < 0.0001
Hippocampus	l -28 -34 -14	5.16	F(5.46,229.47) = 19.0, P < 0.0001	F(1,43) = 70.7, P < 0.0001	F(1,43) = 31.8, P < 0.0001
	r 26 -18 20	5.78	F(2.02,84.51) = 5.6, P < 0.01	F(1,43) = 11.2, P < 0.01	F(1,43) = 8.0, P < 0.01
Precuneus	l -4 58 16	6.75	F(5.11,214.42) = 28.8, P < 0.0001	F(1,43) = 97.6, P < 0.01	F(1,43) = 34.02, P < 0.0001

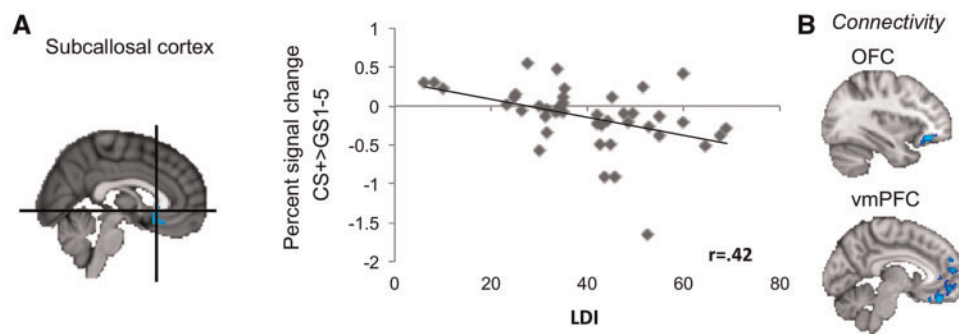


Fig. 4. Pattern separation and neural generalization. (A) Correlation between behavioral pattern separation (LDI) and subcallosal cortex activation for the contrast CS⁺>GS1-GS5. (B) Functional connectivity between the subcallosal cortex and the OFC/ventromedial prefrontal cortex (vmPFC).

response to the GSs compared with the CS⁺ in the subcallosal cortex. No significant associations between LDI and hippocampal activation were observed. Furthermore, the contrasts CS⁺ > GS1 and whole-brain analyses did not reveal any further associations. An exploratory PPI analysis to assess functional connectivity with the subcallosal seed revealed positive functional connectivity with the orbitofrontal cortex (OFC)/avmPFC ([-28 38 -12], Z = 3.81; [-10 50 -12], Z = 3.46) (see Figure 4).

Discussion

This is the first study to demonstrate a link between behavioral pattern separation and the neurobehavioral mechanisms of fear generalization in humans. Lower pattern separation was linked to an increased expectancy of threat, and to decreased activation in the subcallosal cortex during the presentation of GS. The subcallosal cortex showed positive functional connectivity with the OFC/vmPFC during fear generalization.

Generalization gradients were observed in the behavioral data, both for fear and shock expectancy scores. These scores increased as GS became more similar to the conditioned stimulus. This finding is consistent with other studies on fear generalization in humans (Vervliet et al., 2006; van Meurs et al., 2014). Moreover, enhanced fear generalization was related to lower behavioral pattern separation performance. More specifically, pattern separation performance was associated with generalization of shock expectancy data, but not fear ratings. Shock expectancy is a more cognitive expression of threat anticipation, reflecting declarative knowledge of stimulus contingencies (Sevenster et al., 2012; van Well et al., 2012). Our results suggest

that lower pattern separation abilities are related increased estimation of receiving a shock, but not to enhanced feelings of fear when processing ambiguous stimuli. Furthermore, the data of this study imply that cognitive and emotional expressions of fear are independent and rely on different response systems. This is in line with previous research providing evidence for dissociation between cognitive expressions of fear (i.e. skin conductance responses and stimulus contingency awareness) and affective expressions of fear (i.e. self-reported anxiety and startle responses) (Soeter and Kindt, 2010, 2012). The association of behavioral pattern separation with this cognitive expression of threat processing, but not with subjective fear ratings, could be driven by the cognitive, non-emotional nature of the behavioral pattern separation task. Of note, the procedural differences in obtaining the scores (during or after the task phase) may also have contributed to the difference in findings.

At the neural level, lower behavioral pattern separation was linked to reduced activation in the subcallosal cortex during the presentation of GS. This region was functionally connected to the OFC and the avmPFC. Animal and human neuroimaging studies have established that these regions are involved in safety processing, fear inhibition, implicit emotion regulation and threat appraisal (Greenberg et al., 2013a; Etkin et al., 2015; Fullana et al., 2016), by exerting top-down control over brain areas involved in threat processing and fear expression. A large number of studies show that these regions become less active when threat stimuli (CS⁺) are processed and increase in activity when safety cues (CS⁻) are presented (Greenberg et al., 2013a; Lissek et al., 2013; Etkin et al., 2015; Fullana et al., 2016). Moreover, results of numerous structural and functional neuroimaging studies support evidence that dysfunction of these prefrontal

regions represent a pathogenic marker of clinical anxiety (Milad and Rauch, 2007; Myers-Schulz and Koenigs, 2012). PTSD patients show reduced activation in these regions during threat processing and fear extinction (Milad et al., 2008; Hayes et al., 2012). Furthermore, recent studies show that in patients with generalized anxiety disorder, the vmPFC's fear inhibition function is deficient, resulting in enhanced fear reactivity in the context of fear generalization (Greenberg et al., 2013b; Cha et al., 2014). Yet, whether the distinct vmPFC substructures, i.e. the subcallosal cortex and avmPFC, exert different roles during threat anticipation needs to be further investigated. The findings of this study suggest that lower pattern separation functioning can be associated with reduced engagement of fear inhibition processes in the vmPFC, and enhanced generalization of threat expectancies.

Our functional MRI data corroborate previous findings on the neural correlates of fear generalization (Lissek et al., 2013; Dunsmoor and Paz, 2015). Positive neural generalization gradients, reflecting increased activation as GS become more similar to the CS⁺, were detected in the insula, ACC, and VTA and thalamus. These regions play a substantial role in the fear circuitry, and are well known for their contribution to threat processing and fear conditioning (Dunsmoor and Paz, 2015; Fullana et al., 2016). Besides the vmPFC and subcallosal cortex, the hippocampi and precuneus showed negative neural generalization gradients. The negative generalization gradient observed in the hippocampi is in line with recent studies employing cued delay conditioning/generalization procedures (Lissek et al., 2013; Onat and Büchel, 2015; Fullana et al., 2016). The hippocampus is involved in safety signal learning and conscious contingency awareness during threat processing and fear learning (Jovanovic et al., 2012; Lueken et al., 2014; Fullana et al., 2016), and is thought to contribute to fear discrimination processes due to its essential role in pattern separation (Clelland et al., 2009; Aimone et al., 2011; Sahay et al., 2011). Activation in the hippocampi increased as stimuli exhibited lower perceptual similarity to the CS⁺, which could be indicative of pattern separation mechanisms. For stimuli with higher perceptual overlap to the CS⁺, pattern separation might not be initiated, reflected by increased deactivation in the hippocampus. However, no relationship between behavioral pattern separation abilities and activation in the hippocampus during fear generalization was found. This could be explained by the fact that our fMRI task was a validated task designed to assess generalization gradients in behavioral and neural data, and was not specifically designed to capture pattern separation mechanisms. It is possible that the observed hippocampal activation rather reflects safety signal processing, as hippocampal deactivations were greater for (potentially) threatening stimuli than safety stimuli.

The MST taxing pattern separation was assessed in a neutral, non-threatening state, with non-emotional stimuli. Our findings therefore suggest that there are cognitive/perceptual processes unrelated to emotion that influence levels of fear generalization. Results of recent studies nonetheless indicate that perceptual discrimination abilities may decrease during threatening or aversive conditions (Resnik et al., 2011; Dunsmoor and Paz, 2015). Fear learning diminishes perceptual discrimination between CS and GS, thereby inducing fear generalization (Struyf et al., 2015). A recent study further revealed that pattern separation is reduced when retrieval occurs in a threat context, after being encoded during threat (Balderston et al., 2015). This study demonstrated associations between behavioral pattern separation in a neutral context and fear generalization. These associations might have been stronger when pattern separation performance was tested

within a threat condition. Future studies could focus on relating pattern separation performance during threat and fear generalization. Of note, several past studies provide evidence that fear generalization is not merely passively driven by perceptual discrimination or pattern separation abilities (Onat and Büchel, 2015). Factors such as the emotional intensity or ambiguity of the GS, and intolerance to uncertainty are thought to contribute to fear generalization as well (Dunsmoor et al., 2009; Nelson et al., 2015; Onat and Büchel, 2015; Struyf et al., 2015; Morriss et al., 2016). Future studies could assess how these different factors are integrated into a generalized fear response, and how these factors influence generalization with respect to cognitive versus emotional expressions of fear.

It should be noted that details of events stored in episodic memory decay as time passes once memories become less independent on the hippocampus and are stored in the cortex (Wiltgen and Silva, 2007). This time-dependent loss of details regarding threatening events may result in a decreased ability to discriminate between a novel, safe context and a stored threatening context, thereby making fear memories prone to generalize over time (Besnard and Sahay, 2015; Jasnow et al., 2016; Poulos et al., 2016). Furthermore, individuals with PTSD or excessive anxiety may rely more on familiarity than recollection when retrieving remote memories, contributing to enhanced threat uncertainty (Dolcos, 2013). In the current experiment, the CS⁺ and GS were sequentially shown. Future studies focusing on the time-dependent nature of generalization and the underlying process of pattern separation could add to our understanding of generalization in the etiology of anxiety disorders and PTSD.

Validated measures were used to tax pattern separation and fear generalization, and relationships were explored within the established fear circuitry. However, some limitations are that psychophysiological measures, such as skin conductance or fear-potentiated startle responses, were not included as additional measures of threat anticipation. Furthermore, this study was conducted in a healthy volunteer sample. Therefore, we were not able to test whether overgeneralization in clinical anxiety is related to lower pattern separation abilities. Future patient studies in PTSD and patients with anxiety disorders are warranted to further test these hypotheses. In addition, future studies could be directed toward assessing the link between the neural networks of pattern separation and fear generalization.

In conclusion, our findings show that low behavioral pattern separation abilities can be related to enhanced generalization of US expectancies, but not to generalization of fear ratings. These results indicate that pattern separation abilities may influence threat value estimation of stimuli resembling a threat stimulus. Furthermore, the results of this study provide novel insights into the relationship between pattern separation and fear generalization and inhibition mechanisms on a neural level, specifically in the subcallosal cortex. Our results suggest that low pattern separation abilities could possibly contribute to fear overgeneralization, as seen in PTSD and anxiety disorders. Ultimately, targeting pattern separation may represent a novel avenue to treat threat overestimation in these disorders.

Funding and disclosures

This study was funded by a research grant from Stichting de Weijerhorst.

Supplementary data

Supplementary data are available at SCAN online.

Conflict of interest. None declared.

References

- Aimone, J.B., Deng, W., Gage, F.H. (2011). Resolving new memories: a critical look at the dentate gyrus, adult neurogenesis, and pattern separation. *Neuron* 70(4), 589–96.
- Andersson, J.L., Jenkinson, M., Smith, S. (2007). Non-linear registration, aka Spatial normalisation FMRIB technical report TR07JA2. FMRIB Analysis Group of the University of Oxford 2, 1–21.
- Bakker, A., Kirwan, C.B., Miller, M., Stark, C.E. (2008). Pattern separation in the human hippocampal CA3 and dentate gyrus. *Science* 319(5870), 1640–2.
- Balderston, N.L., Mathur, A., Adu-Brimpong, J., Hale, E.A., Ernst, M., Grillon, C. (2015). Effect of anxiety on behavioural pattern separation in humans. *Cognition and Emotion* 31, 238–48.
- Besnard, A., Sahay, A. (2015). Adult hippocampal neurogenesis, fear generalization, and stress. *Neuropsychopharmacology* 41(1), 24–44.
- Cha, J., Carlson, J.M., DeDora, D.J., Greenberg, T., Proudfit, G.H., Mujica-Parodi, L.R. (2014). Hyper-reactive human ventral tegmental area and aberrant mesocorticolimbic connectivity in overgeneralization of fear in generalized anxiety disorder. *The Journal of Neuroscience* 34(17), 5855–60.
- Clelland, C., Choi, M., Romberg, C., et al. (2009). A functional role for adult hippocampal neurogenesis in spatial pattern separation. *Science* 325(5937), 210–3.
- Cullen, P.K., Gilman, T.L., Winiecki, P., Riccio, D.C., Jasnow, A.M. (2015). Activity of the anterior cingulate cortex and ventral hippocampus underlie increases in contextual fear generalization. *Neurobiology of Learning and Memory* 124, 19–27.
- Deuker, L., Doeller, C.F., Fell, J., Axmacher, N. (2014). Human neuroimaging studies on the hippocampal CA3 region—integrating evidence for pattern separation and completion. *Frontiers in Cellular Neuroscience* 8,
- Dolcos, F. (2013). Linking enhancing and impairing effects of emotion—the case of PTSD. *Frontiers in Integrative Neuroscience* 7, 26.
- Dunsmoor, J.E., Mitroff, S.R., LaBar, K.S. (2009). Generalization of conditioned fear along a dimension of increasing fear intensity. *Learning & Memory* 16(7), 460–9.
- Dunsmoor, J.E., Paz, R. (2015). Fear generalization and anxiety: behavioral and neural mechanisms. *Biological Psychiatry* 78(5), 336–43.
- Dymond, S., Dunsmoor, J.E., Vervliet, B., Roche, B., Hermans, D. (2014). Fear generalization in humans: systematic review and implications for anxiety disorder research. *Behavior Therapy* 46(5), 561–82
- Etkin, A., Büchel, C., Gross, J.J. (2015). The neural bases of emotion regulation. *Nature Reviews Neuroscience* 16(11), 693–700.
- Fullana, M., Harrison, B., Soriano-Mas, C., et al. (2016). Neural signatures of human fear conditioning: an updated and extended meta-analysis of fMRI studies. *Molecular Psychiatry* 21(4), 500–8.
- Greenberg, T., Carlson, J.M., Cha, J., Hajcak, G., Mujica-Parodi, L.R. (2013a). Neural reactivity tracks fear generalization gradients. *Biological Psychology* 92(1), 2–8.
- Greenberg, T., Carlson, J.M., Cha, J., Hajcak, G., Mujica-Parodi, L.R. (2013b). Ventromedial prefrontal cortex reactivity is altered in generalized anxiety disorder during fear generalization. *Depression and Anxiety* 30(3), 242–50.
- Hayes, J.P., VanElzaker, M.B., Shin, L.M. (2012). Emotion and cognition interactions in PTSD: a review of neurocognitive and neuroimaging studies. *Frontiers in Integrative Neuroscience* 6, 89.
- Jasnow, A.M., Lynch, J.F., Gilman, T.L., Riccio, D.C. (2016). Perspectives on fear generalization and its implications for emotional disorders. *Journal of Neuroscience Research* 95(3), 821–35.
- Jenkinson, M., Bannister, P., Brady, M., Smith, S. (2002). Improved optimization for the robust and accurate linear registration and motion correction of brain images. *Neuroimage* 17(2), 825–41.
- Jovanovic, T., Kazama, A., Bachevalier, J., Davis, M. (2012). Impaired safety signal learning may be a biomarker of PTSD. *Neuropharmacology* 62(2), 695–704.
- Kaczurkin, A.N., Burton, P.C., Chazin, S.M., et al. (2016). Neural substrates of overgeneralized conditioned fear in PTSD. *American Journal of Psychiatry* 174(2), 125–34.
- Kheirbek, M.A., Klemenhagen, K.C., Sahay, A., Hen, R. (2012). Neurogenesis and generalization: a new approach to stratify and treat anxiety disorders. *Nature Neuroscience* 15(12), 1613–20.
- Li, F., Wang, L.P., Shen, X., Tsien, J.Z. (2010). Balanced dopamine is critical for pattern completion during associative memory recall. *PLoS One* 5(10), e15401.
- Lissek, S. (2012). Toward an account of clinical anxiety predicated on basic, neurally mapped mechanisms of pavlovian fear-learning: the case for conditioned overgeneralization. *Depression and Anxiety* 29(4), 257–63.
- Lissek, S., Bradford, D.E., Alvarez, R.P., et al. (2013). Neural substrates of classically conditioned fear-generalization in humans: a parametric fMRI study. *Social Cognitive and Affective Neuroscience* 9(8), 1134–42.
- Lopresto, D., Schipper, P., Homberg, J.R. (2016). Neural circuits and mechanisms involved in fear generalization: implications for the pathophysiology and treatment of posttraumatic stress disorder. *Neuroscience & Biobehavioral Reviews* 60, 31–42.
- Lueken, U., Straube, B., Konrad, C., et al. (2014). Neural substrates of treatment response to cognitive-behavioral therapy in panic disorder with agoraphobia. *American Journal of Psychiatry* 170, 1345–55.
- McHugh, T.J., Jones, M.W., Quinn, J.J., et al. (2007). Dentate gyrus NMDA receptors mediate rapid pattern separation in the hippocampal network. *Science* 317(5834), 94–9.
- Messman-Moore, T.L., Walsh, K.L., DiLillo, D. (2010). Emotion dysregulation and risky sexual behavior in revictimization. *Child Abuse & Neglect* 34(12), 967–76.
- Milad, M.R., Orr, S.P., Lasko, N.B., Chang, Y., Rauch, S.L., Pitman, R.K. (2008). Presence and acquired origin of reduced recall for fear extinction in PTSD: results of a twin study. *Journal of Psychiatric Research* 42(7), 515–20.
- Milad, M.R., Rauch, S.L. (2007). The role of the orbitofrontal cortex in anxiety disorders. *Annals of the New York Academy of Sciences* 1121(1), 546–61.
- Morriss, J., Macdonald, B., van Reekum, C.M. (2016). What is going on around here? Intolerance of uncertainty predicts threat generalization. *PLoS One* 11(5), e0154494.
- Myers-Schulz, B., Koenigs, M. (2012). Functional anatomy of ventromedial prefrontal cortex: implications for mood and anxiety disorders. *Molecular Psychiatry* 17(2), 132–41.
- Nakashiba, T., Cushman, J.D., Pelkey, K.A., et al. (2012). Young dentate granule cells mediate pattern separation, whereas old granule cells facilitate pattern completion. *Cell* 149(1), 188–201.
- Nelson, B.D., Weinberg, A., Pawluk, J., Gawlowska, M., Proudfit, G.H. (2015). An event-related potential investigation of fear generalization and intolerance of uncertainty. *Behavior Therapy* 46(5), 661–70.
- Neunuebel, J.P., Knierim, J.J. (2014). CA3 retrieves coherent representations from degraded input: direct evidence for CA3

- pattern completion and dentate gyrus pattern separation. *Neuron* **81**(2), 416–27.
- Onat, S., Büchel, C. (2015). The neuronal basis of fear generalization in humans. *Nature Neuroscience* **18**, 1811–8.
- Overbeek, I., Schruers, K., Griez, E. (1999) *Mini International Neuropsychiatric Interview: Nederlandse Versie 5.0.0, DSM-IV [Dutch Version]*. Maastricht, The Netherlands: Universiteit Maastricht.
- Poulos, A.M., Mehta, N., Lu, B., et al. (2016). Conditioning-and time-dependent increases in context fear and generalization. *Learning & Memory* **23**(7), 379–85.
- Resnik, J., Sobel, N., Paz, R. (2011). Auditory aversive learning increases discrimination thresholds. *Nature Neuroscience* **14**(6), 791–6.
- Sahay, A., Scobie, K.N., Hill, A.S., et al. (2011). Increasing adult hippocampal neurogenesis is sufficient to improve pattern separation. *Nature* **472**(7344), 466–70.
- Sevenster, D., Beckers, T., Kindt, M. (2012). Retrieval per se is not sufficient to trigger reconsolidation of human fear memory. *Neurobiology of Learning and Memory* **97**(3), 338–45.
- Smith, S.M. (2000) BET: brain extraction tool. FMRIB TR00SMS2b, Oxford Centre for Functional Magnetic Resonance Imaging of the Brain), Department of Clinical Neurology, Oxford University, John Radcliffe Hospital, Headington, UK.
- Smith, S.M., Jenkinson, M., Woolrich, M.W., et al. (2004). Advances in functional and structural MR image analysis and implementation as FSL. *Neuroimage* **23**, S208–19.
- Soeter, M., Kindt, M. (2010). Dissociating response systems: erasing fear from memory. *Neurobiology of Learning and Memory* **94**(1), 30–41.
- Soeter, M., Kindt, M. (2012). Erasing fear for an imagined threat event. *Psychoneuroendocrinology* **37**(11), 1769–79.
- Stark, S.M., Yassa, M.A., Lacy, J.W., Stark, C.E. (2013). A task to assess behavioral pattern separation (BPS) in humans: data from healthy aging and mild cognitive impairment. *Neuropsychologia* **51**(12), 2442–9.
- StataCorp (2013) *Stata Statistical Software: Release 13*. College Station, TX: StataCorp LP.
- Struyf, D., Zaman, J., Vervliet, B., Van Diest, I. (2015). Perceptual discrimination in fear generalization: Mechanistic and clinical implications. *Neuroscience & Biobehavioral Reviews* **59**, 201–7.
- van Meurs, B., Wiggert, N., Wicker, I., Lissek, S. (2014). Maladaptive behavioral consequences of conditioned fear-generalization: a pronounced, yet sparsely studied, feature of anxiety pathology. *Behaviour Research and Therapy* **57**, 29–37.
- van Well, S., Visser, R.M., Scholte, H.S., Kindt, M. (2012). Neural substrates of individual differences in human fear learning: evidence from concurrent fMRI, fear-potentiated startle, and US-expectancy data. *Cognitive, Affective, & Behavioral Neuroscience* **12**(3), 499–512.
- Vervliet, B., Vansteenwegen, D., Eelen, P. (2006). Generalization gradients for acquisition and extinction in human contingency learning. *Experimental Psychology* **53**(2), 132–42.
- Wager, T.D., Nichols, T.E. (2003). Optimization of experimental design in fMRI: a general framework using a genetic algorithm. *Neuroimage* **18**(2), 293–309.
- Wiltgen, B.J., Silva, A.J. (2007). Memory for context becomes less specific with time. *Learning & Memory* **14**(4), 313–7.
- Woolrich, M.W., Ripley, B.D., Brady, M., Smith, S.M. (2001). Temporal autocorrelation in univariate linear modeling of fMRI data. *Neuroimage* **14**(6), 1370–86.
- Xu, W., Südhof, T.C. (2013). A neural circuit for memory specificity and generalization. *Science* **339**(6125), 1290–5.
- Yassa, M.A., Stark, C.E. (2011). Pattern separation in the hippocampus. *Trends in Neurosciences* **34**(10), 515–25.